JCI insight

RESEARCH ARTICLE

Tumor-infiltrating lymphocytes are dynamically desensitized to antigen but are maintained by homeostatic cytokine

Bijan Boldajipour,[1] Amanda Nelson,[1] and Matthew F. Krummel[1,2]

[1]Department of Pathology and [2]Biological Imaging Development Center, UCSF, San Francisco, California, USA.

T cells that enter tumors are largely tolerized, but how that process is choreographed and how the ensuing "dysfunctional" tumor-infiltrating lymphocytes (TILs) are maintained are poorly understood and are difficult to assess in spontaneous disease. We exploited an autochthonous model of breast cancer for high-resolution imaging of the early and later stages of tumor residence to understand the relationships between cellular behaviors and cellular phenotypes. "Dysfunctional" differentiation began within the first days of tumor residence with an initial phase in which T cells arrest, largely on tumor-associated macrophages. Within 10 days, cellular motility increased and resembled a random walk, suggesting a relative absence of TCR signaling. We then studied the concurrent and apparently contradictory phenomenon that many of these cells express molecular markers of activation and were visualized undergoing active cell division. We found that whereas proliferation did not require ongoing TCR/ZAP70 signaling, instead this is driven in part by intratumoral IL-15 cytokine. Thus, TILs undergo sequential reprogramming by the tumor microenvironment and are actively retained, even while being antigen insensitive. We conclude that this program effectively fills the niche with ineffective yet cytokine-dependent TILs, and we propose that these might compete with new clones, when they arise.

Introduction

The "Hellstrom paradox" defines the coexistence of progressively growing tumors and tumor-infiltrating T cells (TILs) and suggests that tumor-specific T cells are rendered unresponsive to the cancer, despite being amplified (1). It is now well recognized that $CD8^+$ TILs within progressing, solid tumors and metastatic lesions accumulate and frequently express high levels of "exhaustion" markers (2), including inhibitory receptors (e.g., PD1, LAG3, 2B4, TIM3, CTLA4). Further, these cells are defective in their ability to produce effector cytokines (TNF-α, IFN-γ, and IL-2) and/or have lost the capacity to proliferate in response to antigens (3–6). These hallmarks of dysfunction have been attributed to a number of defined and hypothesized factors within established tumors, broadly described as an immunosuppressive tumor microenvironment (TME). The steps leading to the conversion of incoming T cells to a "dysfunctional" state is thus a subject of great interest, and we sought novel ways to study high- and low-affinity clones as they entered and were conditioned by this TME.

Tumor-antigen reactive $CD8^+$ T cells adopted into mice bearing spontaneously arising and immunoevasive tumors are efficiently expanded in draining lymph nodes (4, 7, 8) and subsequently traffic to tumor. Such expansion is also presumed to precede establishment of TILs in human cancer, since T cells that bear tumor antigen-specific T cell receptors (TCRs) are vastly overrepresented within the tumor and indeed within the blood of afflicted individuals (9, 10). With the exception of some ectopic models in which TMEs may be different than those in tumors that form more naturally, adoptive transfer and subsequent clonal expansion of T cells are insufficient to mediate tumor clearance (11–13). Similarly, adoption of high numbers of expanded and activated T cells in human patients is ultimately only sporadically successful as a monotherapy (13). Based on this empirical data, it is supposed that the TME converts incoming cytotoxic T lymphocytes (CTLs) into dysfunctional TILs, but tracking the steps in this process within the TME has not hitherto been possible.

T cells migrate as part of their surveillance program (14) and profound TCR activation leads to an arrest of T cell migration, reducing overall speed (15, 16). T cell arrest in vivo has thus been established to

Conflict of interest: The authors have declared that no conflict of interest exists.

Submitted: June 27, 2016
Accepted: October 25, 2016
Published: December 8, 2016

Reference information:
JCI Insight. 2016;1(20):e89289.
doi:10.1172/jci.insight.89289.

be an indicator of T cell recognition of antigen-presenting cells (APCs) (17, 18), although we and others have shown that TCR triggering can also occur without substantial stopping (19–21) and lead to a "motile synapse" (or sometimes "kinapse"). Other factors may also modulate motility; integrins may either speed up (22) or slow down (23) migration, and chemokines can either induce faster scanning (22) or "tether" cells in place (24). Regardless, scanning for antigens (motility) and formation of stable interactions (arrest) remain key features of T cell biology, and to understand them is a key prelude to understanding deficits in detection of antigens versus response to cues (14).

In previous live-imaging studies, we and others have shown that effector CD8 T cells, shortly after TME entry, are found in an arrested motility state, in association with marginating myeloid APC populations (4, 7, 11, 12). We previously demonstrated that the myeloid APC populations that engage incoming CTLs in vivo also mediate a stable synaptic contact with CTLs in vitro, a contact that induced calcium transients within the T cells that were equivalent to those produced by stimulatory APCs (4). However, when encountering these types of macrophages, T cells lost or retained cytotoxic function and proliferation, respectively (4, 7). In tumors, the long-term effect of encountering these APC subtypes on T cell behavior, and how this relates to T cell dysfunction, has not been studied. Do T cells continue to stably engage these APCs with the same frequency as time progresses, for example, as a condition to maintain tolerance? How does activation status change over time relative to the formation of initial T cell–tumor-associated macrophage (T cell–TAMs) contacts? And if these contacts disable T cell function, what sustains T cells there?

Here, we used an intravital live-imaging approach to study the evolving behavior and reprogramming of high-affinity T cells after entry into the TME using a spontaneous breast cancer model with a long development time and a defined tumor antigen (4). This tumor model appears to recapitulate the accumulation of tumor-reactive, yet defective, TILs that are characteristic of human disease. Imaging directly into the tumor during different times of T cell residency, we found that T cells that have been exposed to TMEs for a long time exhibit migration patterns that suggest a cessation of the prolonged APC interactions that were observed upon initial entry. This change corresponds with intratumoral downregulation of the transcription factor NR4A1/NUR77 as well as cytotoxic cytokines and surface-expressed activation markers. Despite this, we found that TILs were dividing in the TME, which was not mediated by TCR signaling, but instead relied in part on the cytokine IL-15. We have thus determined that the TME first engages T cells and then retains them in a dysfunctional state with reduced TCR engagement, in part by local production of homeostatic cytokine.

Results

Progression of T cell motility in the TME. To study the evolution of T cell recognition of tumors, at the single-cell level and in real time, we transferred genetically labeled naive ovalbumin-specific OT-I $CD8^+$ T cells into PyMT-ChOVA mice that express ovalbumin as a tumor antigen and observed their migration using 2-photon intravital microscopy. As previously reported (4), we found OT-I cells in significant numbers in tumors as early as 4 days after transfer, which we considered as "recent arrivals." To compare motility of these with the existing TILs that had populated the tumor during its prolonged development, we intercrossed the *Pymtchova* allele with a *Cd2rfp* allele (25), which marks all endogenous T cells with the red fluorescent protein (Figure 1, A–D). We organized these experiments so that both cell types were observed in the exact same imaging runs and noted that these cells occupied the same territory. As previously reported (4, 12), the majority of recent arrivals into the tumor margins exhibited short 2-hour tracks (Figure 1, B and C) and migrated at speeds of between 1 and 2 μm/min, with pronounced arrest coefficients (Figure 1D and Supplemental Video 1; supplemental material available online with this article; doi:10.1172/jci.insight.89289DS1). In contrast, endogenous T cells had longer tracks when similarly plotted, migrated approximately twice as fast, and exhibited little arrest — frequently passing arrested OT-I T cells. Together, this suggests that the observed motility differences were not the effect of occupying distinct microenvironments (Figure 1, B and C, and Supplemental Video 1).

Since endogenous T cells against spontaneous tumors typically have low-affinity TCRs, often due to expression of the prominent tumor-associated self antigens in the thymus (4), we investigated whether different TCR affinities could explain the difference in motility observed. We thus simultaneously transferred equal numbers of OT-I T cells, which express a high-affinity TCR for OVA, with OT-3 T cells, which express a TCR with much lower affinity for the same peptide (26), and compared their migration after tissue entry. Although we found many fewer OT-3 T cells in tumors (Figure 1H), their motility behavior closely matched that of OT-I T cells (Figure 1, E–H, and Supplemental Video 2). Thus, while that variation in TCR strength clearly affects clonal expansion, it is not a significant variable for influencing intratumoral T cell motility at this time point.

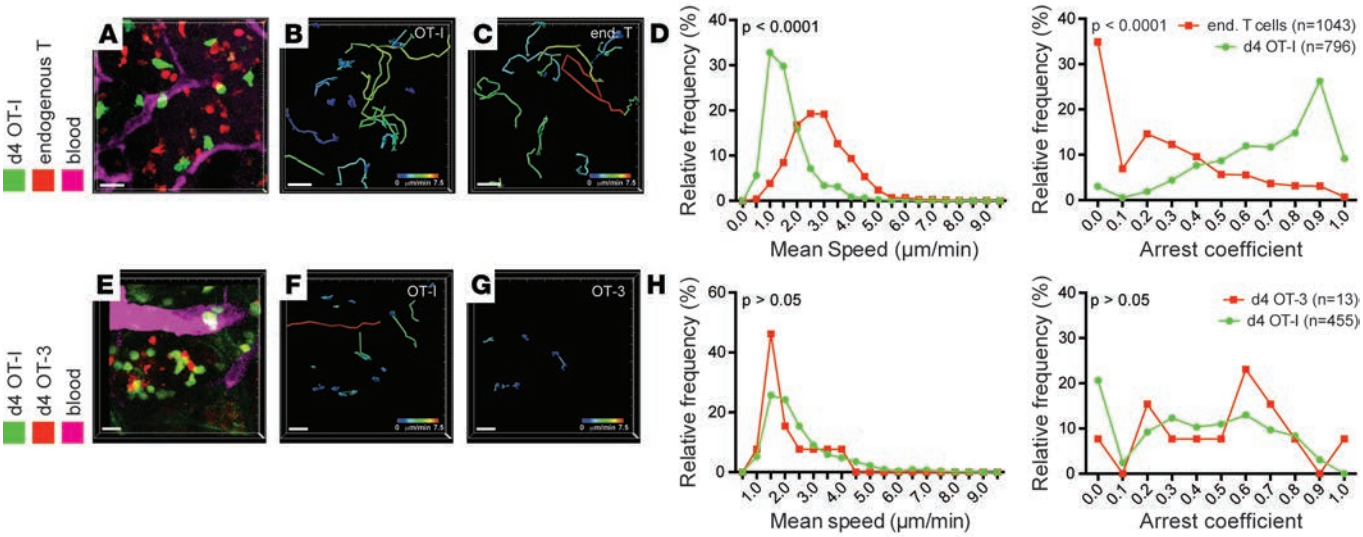

Figure 1. T cell arrest upon arrival to the tumor is independent of TCR affinity. (**A–D**) Migration parameters of high-affinity T cells in tumors upon arrival at the tumor site compared to endogenous T cells. (**A–C**) Representative video snapshot and migratory paths of high-affinity T cells and endogenous T cells over 2 hours, color-coded for mean track speed. CD11cYFP channel not displayed for ease of projection (see also Supplemental Video 1). (**D**) Kolmogorov-Smirnov analysis of the distribution of average migration speed and arrest coefficients. Data are representative of 6 experiments. (**E–H**) Migration parameters of high-affinity OT-I T cells compared with low-affinity OT-3 T cells upon arrival at the tumor site. (**E–G**) Representative video snapshot and migratory paths of high-affinity OT-I T cells and low-affinity OT-3 T cells over 2 hours, color-coded for mean track speed. (**H**) Kolmogorov-Smirnov analysis of the distribution of average migration speed and arrest coefficients. Due to the low numbers of OT-3 cells, data are pooled from 3 experiments. Scale bars: 20 μm.

An alternate explanation for the differences in motility between recent arrivals and endogenous T cells is the residence time of the cells in the TME. Whereas endogenous T cells have been exposed to tumor antigen for several weeks or months, OT-I T cells have just entered. The altered migration may therefore indicate a maturation or adaption of T cells to the tumor site. To test this idea, we analyzed the migration of OT-I T cells 14 days after transfer into PyMT-ChOVA/CD2-RFP mice, in which endogenous T cells were again compared in the same imaging period (Figure 2, A–D, and Supplemental Video 3). In these comparisons, tumor-experienced OT-I T cells were found to exhibit long tracks similar to endogenous T cells, with speed and arrest coefficients indistinguishable from endogenous T cells (Figure 2, B–D). This suggests that long-term exposure to TMEs results in a relative inability to arrest. To confirm that the switch from arrest to migration was a cell-intrinsic process, and not caused by an altered microenvironment (e.g., elimination of tumor dendritic cells by high-affinity T cells), we compared the migration of tumor-experienced OT-I T cells to that of OT-I T cells that have recently arrived within the same animal (Figure 2, E–H, and Supplemental Video 4). Again, recent arrivals had shorter tracks, lower average speeds, and higher arrest coefficients compared with tumor-experienced OT-I cells. We found similarly increased motility already by day 10 (data not shown), but in the interest of consistency, we compared day 4 and day 14 for the remainder of this study. Together, these experiments indicate that T cells undergo reprogramming of their ability to arrest upon exposure to the TME.

Finally, we used imaging to directly observe the degree to which later TILs had available access to the TAM populations that are engaged by early arrivals (day 4–6 in previous studies; ref. 4). In our previous imaging of early TIL interactions in the TME, we had exploited a reporter system consisting of a combination of the *Cx3cr1gfp* (27) and *Cd11ccherry* reporter alleles (28). Based on the relative expression of these reporters, monocyte-derived immature macrophages (TAM1) and mature macrophages (TAM2) can be distinguished from conventional dendritic cells (CD11b/CD103 DC; ref. 7). When we introduced CFP-labeled OT-I T cells into these mice, we determined that tumor-experienced T cells also remained within the tumor tissue and were mostly intermixed in zones containing both TAM1 and TAM2 (Figure 2, I and J) and that the vast majority of them were within 5 μm (less than their cell width) of both of these cell types at any one time (Figure 2K). We conclude that residence time but not access to APC is likely responsible for changes in the motility of TILs.

Dynamic changes in markers of T cell activation associated with tumor residence. Our previous results in vitro indicated that engagement of CTLs by TAMs was paradoxically able to both mediate a stable synapse and to induce proximal calcium signaling, despite being unable to drive proliferation or maintain effector func-

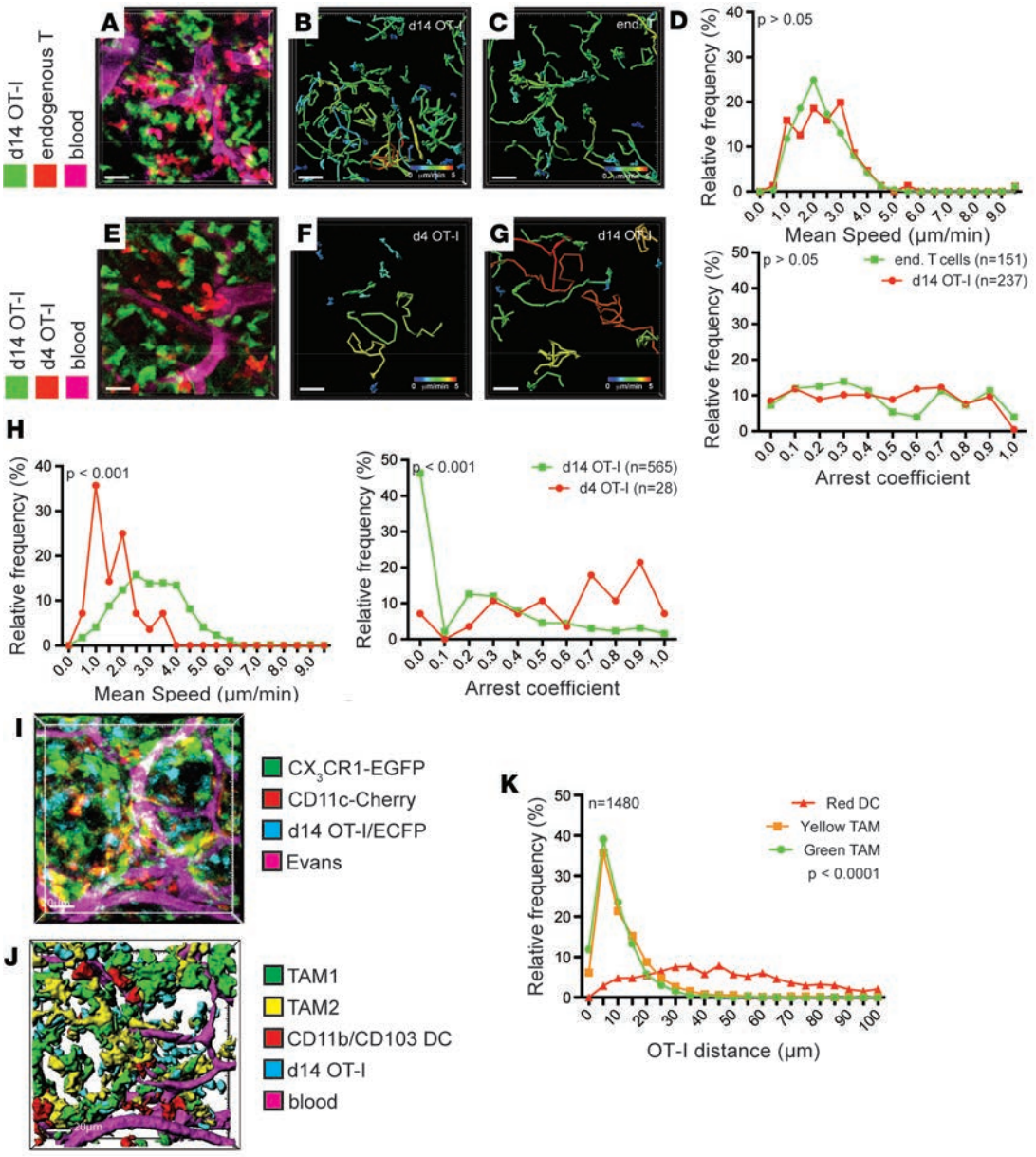

Figure 2. Exposure to tumor environment alters T cell behavior. (**A–D**) Migration parameters of tumor-resident high-affinity T cells compared with endogenous T cells. (**A–C**) Representative video snapshot and migratory paths of high-affinity T cells and endogenous T cells, color-coded for mean track speed over 2 hours. (**D**) Kolmogorov-Smirnov analysis of the distribution of average migration speed and arrest coefficients. Data are representative of 5 experiments. (**E–H**) Comparison of migration parameters of high-affinity T cells upon recent arrival to tumors (red) and after establishing residence (green) within the same animal. (**E–G**) Representative video snapshot and migratory paths of high-affinity T cells upon recent arrival to tumors and after establishing residence, color-coded for mean track speed over 2 hours. (**H**) Kolmogorov-Smirnov analysis of the distribution of average migration speed and arrest coefficients. Data are representative of 5 experiments. (**I**) Snapshot and rendering (**J**) of the localization of high-affinity T cells (blue), CD11b$^+$ TAM1 macrophages (green), CD11c$^+$ TAM2 macrophages (yellow), and dendritic cells (red) 14 days after transfer of OT-I/CFP T cells into PyMT-ChOVA/CX3CR1-EGFP/CD11c-RFP transgenic hosts. Blood vessels were labeled by Evans Blue. (**K**) Representative statistical analysis of the distance of OT-I T cells to the next available APC using a Kruskal-Wallis 1-way ANOVA test. Data are representative of 2 experiments, *n* denotes the numbers of T cells analyzed. Scale bars: 20 μm.

tion (4, 7). We therefore sought to correlate the changes in tissue scanning, seen during tumor residence time, with T cell activation parameters in that same window. Toward this, we first took advantage of the *Nr4a1gfp* allele to measure TCR activity of early and resident OT-I TILs by in situ imaging. As shown in Figure 3, A and B, this demonstrated that while approximately 65% of day 4 TILs were NUR77-GFP pos-

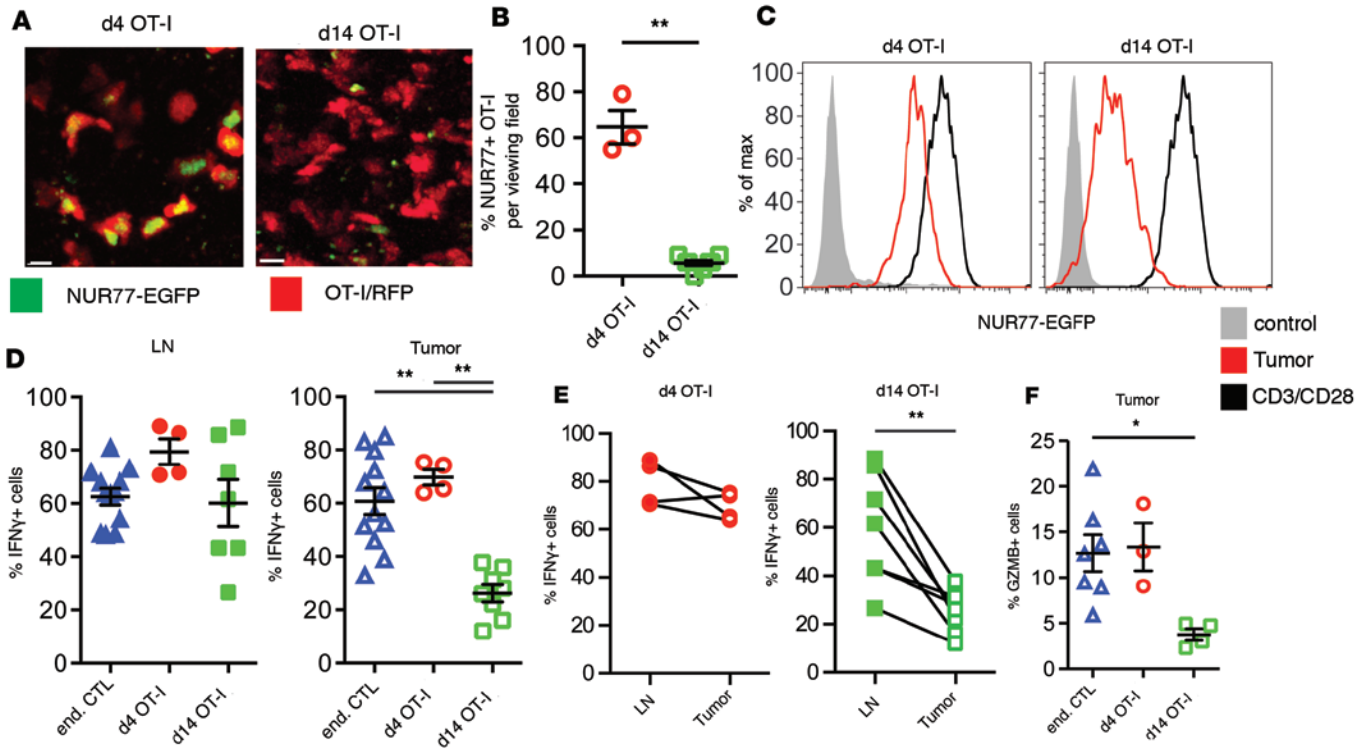

Figure 3. Reduced TCR signaling and effector function in tumor-specific T cells. (**A**) Representative images of OT-I/CD2-RFP/NUR77-EGFP reporter T cells after arrival and after establishing residence in tumors. Scale bars: 10 μm. (**B**) Statistical analysis of the percentage of NUR77-positive T cells in PyMT-ChO-VA tumors using a Mann-Whitney *t* test, $^{**}P < 0.01$. Data are analyzed from multiple tumors analyzed from 2 animals. (**C**) Analysis of the NUR77-EGFP reporter activity in OT-I T cells isolated from tumors (red). In vitro–activated T cells cultured for 24 hours on CD3/CD28-coated plates serve as positive control (black). OT-I/NUR77-EGFP T cells isolated from spleens of naive mice serve as negative control (filled gray histogram). Data are representative of at least 3 experiments. (**D–F**) Analysis of cytokine expression by ex vivo–restimulated CD44^{hi} endogenous CD8^{+} T cells and OT-I T cells at different time points after adoptive transfer. (**D**) Cytokine expression in tumor-draining lymph nodes and tumors of PyMT-ChOVA animals. Statistical analysis was performed using a 1-way ANOVA Kruskal-Wallis test. (**E**) Comparison of cytokine expression in tumor-draining lymph nodes and their corresponding tumors. Samples were analyzed using the Wilcoxon matched-pairs rank test. (**F**) Granzyme B expression in tumor-resident T cells. Statistical analysis was performed using a 1-way ANOVA Kruskal-Wallis test, $^{*}P < 0.05$, $^{**}P < 0.01$.

itive, less than 10% of cells at day 14 were similarly positive. We used flow cytometry to compare the mean NUR77 reporter activity of tumor-derived OT-I against OT-I T cells activated with anti-CD3/anti-CD28 antibodies in vitro and found that, whereas day 4 TILs had approximately 4-fold lower reporter activity than these controls, the day 14 resident TILs were approximately 18-fold lower (Figure 3C). Together, these data strongly suggest reduced TCR signaling with prolonged residence time.

To extend this analysis to measures of effector function, we isolated and assayed lymph node and TILs for their ability to produce IFN-γ. In lymph nodes, both OT-I and endogenous T cells on average retained their ability to produce IFN-γ, independent of their residence time. In tumors, tumor-resident OT-I cells lost IFN-γ expression between day 4 and day 14, whereas the endogenous T cells maintained their IFN-γ production (Figure 3D). When we compared the IFN-γ expression between lymph node and tumor-resident OT-I cells of the same animal, we observed an insignificant reduction in the percentage of cells that were positive for IFN-γ 4 days after transfer but consistently significant reductions in every mouse when compared at day 14 (Figure 3E). Similar to their failure to produce IFN-γ, tumor-experienced OT-I cells also lost the ability to produce the cytotoxic effector molecule granzyme B (GZMB; Figure 3F). This was also reflected by the absence of apoptotic cell death of tumor cells in situ, despite very high numbers of tumor-infiltrating OT-I T cells (data not shown).

Finally, the change in T cell effector phenotype was accompanied by a change in their surface phenotype. We analyzed the expression of several surface markers associated with T cell function (Supplemental Figure 2A). While initially expressed at high levels, OT-I T cells downregulated CD25, CTLA4, and CD160, while PD1 and CD223/LAG3 remained unchanged and 2B4 and TIM3 expression increased. Of note, the expres-

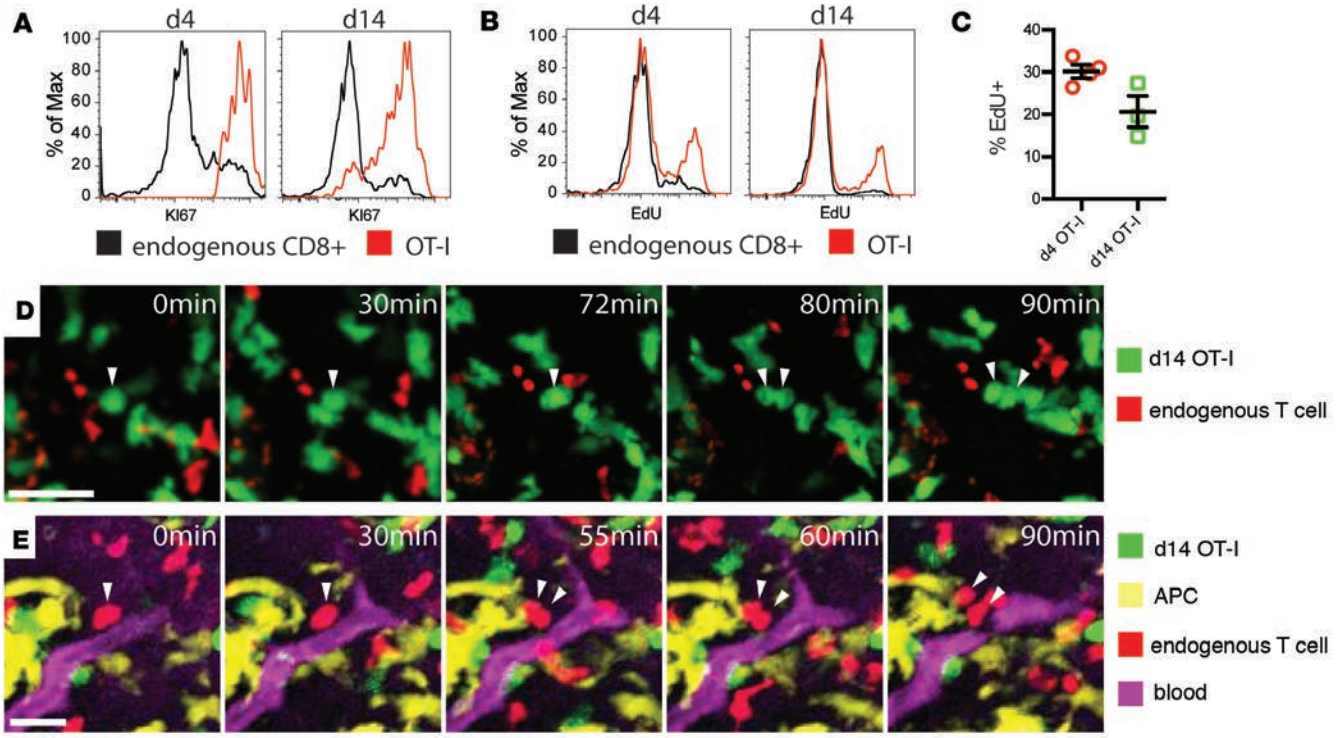

Figure 4. Tumor-resident T cells proliferate in the tumor microenvironment. (**A** and **B**) Expression of KI67 (**A**) and incorporation of EdU during DNA synthesis within 24 hours (**B**) in endogenous CD44^{hi} CD8^{+} T cells (black), or high-affinity T cells (red), after arrival of OT-I T cells to the tumor (left) and after establishing residence (right). (**C**) Statistical analysis of EdU incorporation in several experiments. Mann-Whitney test, $P > 0.05$. (**D** and **E**) Snapshots of time-lapse videos of dividing high-affinity T cells (**D**, green) and endogenous T cells (**E**, red) in tumors of PyMT-ChOVA/CD2-RFP hosts. (**E**) CD11c^{+} antigen-presenting cells (APC, yellow) are visualized by the expression of an additional CD11c-YFP transgene, and blood vessels are labeled by Evans Blue (magenta). Arrows show dividing T cells and their daughter cells. Scale bar: 20 μm.

sion levels of CD25, CTLA4, and SLAM/CD160 in the endogenous T cells mirrored those of tumor-experienced OT-I cells, whereas PD1, LAG3, CD244/2B4, and TIM3 were expressed at higher levels in OT-I cells (Supplemental Figure 1). This discrepancy may represent the effects of especially long prolonged tumor residence. Taken together, these data demonstrate that early arrest of motile TILs on APCs is associated with previous or ongoing T cell activation but that enhanced intratumoral motility coincides with establishment of a "dysfunctional" phenotype, with some features suggesting a lack of ongoing TCR engagement.

In situ antigen-independent cell division of high-affinity T cells in tumors. In the course of staining for exhaustion markers in transferred populations, we made the observation that both recently arrived and tumor-experienced OT-I cells uniformly expressed high levels of KI67, a nuclear marker of cell cycle entry (Figure 4A). To a lesser degree, endogenous CD8^{+} TILs also bore evidence of ongoing cell cycle. While the activation and proliferation of naive T cells in tumors has been reported (29), active proliferation of TILs in situ has not been well recognized to our knowledge. To test whether the day 14 cells were in fact cycling, we transferred OT-I T cells into tumor-bearing PyMT-ChOVA mice and treated animals with the nucleotide analog EdU to mark cells synthesizing DNA and with the S1P receptor inhibitor FTY720 to prevent infiltration of T cells from the lymph node (Figure 4B). Consistent with the other evidence of their activated state, approximately 30% of recently adopted cells incorporated EdU within a 20-hour period, but, surprisingly given the absence of other evidence of their activation, nearly 20% of tumor-experienced OT-I cells also incorporated EdU (Figure 4C). We also typically found endogenous cells undergoing EdU incorporation in these assays, yet at much lower levels. Such a bystander effect may be a result of initial cytokine production by the incoming CTLs, although other possibilities exist. During our imaging runs, we correspondingly found that both endogenous (Figure 4D and Supplemental Video 5) and OT-I (Figure 4E and Supplemental Video 6) T cells were observed undergoing cell division. In sum, these observations defined intratumoral cell-division as a feature of TILs during their initial residence and even after they had ceased to profoundly arrest in the TME.

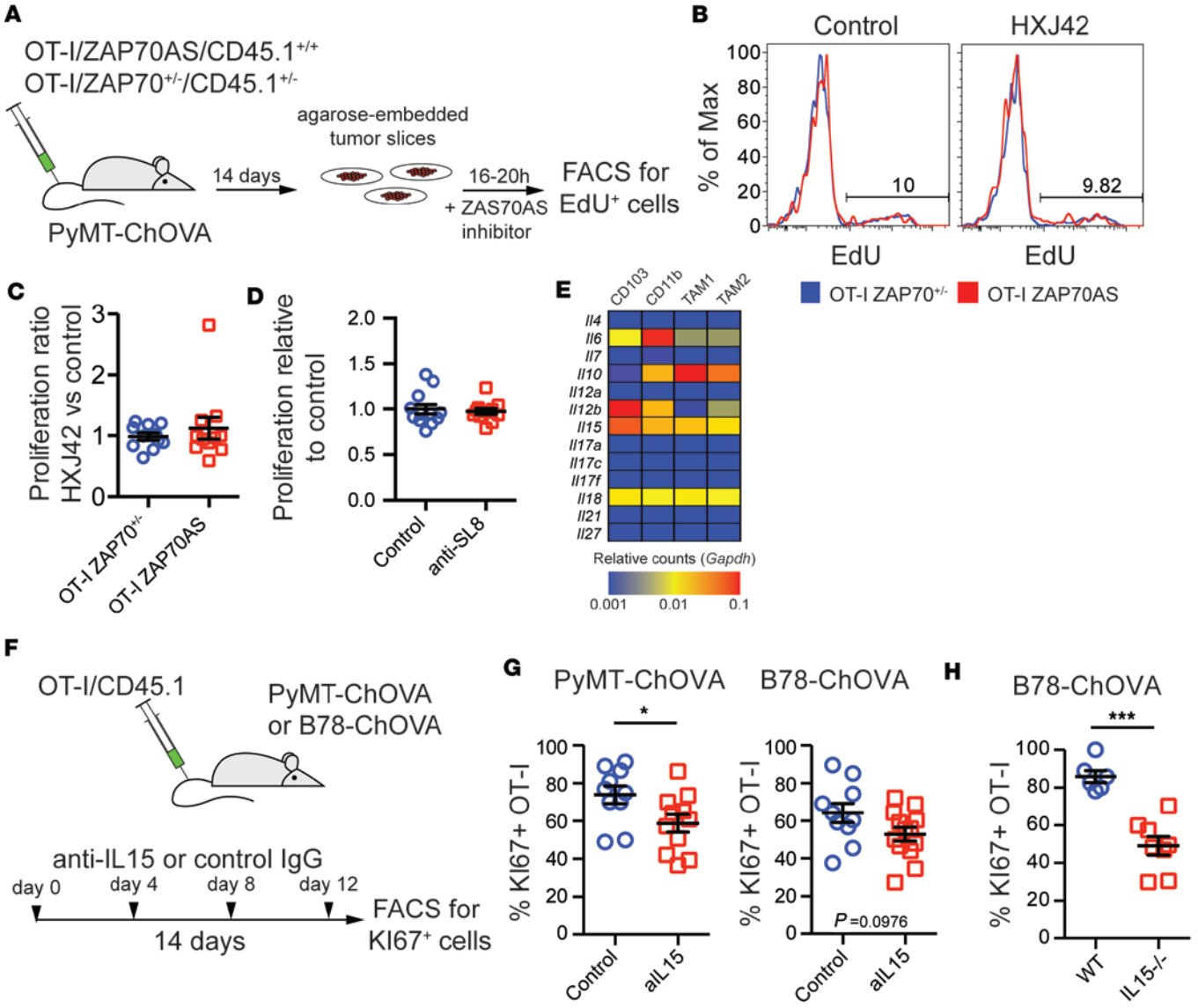

Figure 5. Proliferation of tumor-resident T cells is independent of TCR signaling but partially dependent on IL-15 signaling. (**A**) Schematic of experiments to address TCR dependence of the proliferation of tumor-resident T cells. Genetically marked OT-I T cells expressing either a single copy of wild-type ZAP70 or the HXJ42-sensitive mutant ZAP70AS were transferred to PyMT-ChOVA mice. Fourteen days later, tumor slice cultures were prepared from tumors and incubated for 24 hours in the presence of EdU and either HXJ42 inhibitor or DMSO control. (**B**) Representative analysis of EdU incorporation of inhibitor-resistant OT-I/ZAP70$^{+/-}$ or inhibitor-sensitive OT-I/ZAP70AS T cells in the presence or absence of the inhibitor using flow cytometry. (**C**) The ratio of proliferation in tumor slices incubated with HXJ42 inhibitor over the proliferation in control slices was analyzed using a Mann-Whitney test. $P > 0.05$. Data are pooled from 3 experiments. (**D**) Similar to **A–C**, tumor slices of PyMT-ChOVA mice treated with OT-I T cells were incubated with EdU in absence or presence of an antibody that blocks the MHCI-presented ovalbumin peptide (anti-SL8). EdU incorporation was compared against the average of the control group using a Mann-Whitney test. $P > 0.05$. Data are pooled from 3 experiments. (**E**) Analysis of homeostatic cytokine expression by myeloid cells in the tumor microenvironment. Cytokine RNA expression data from ref. 7 were mined for each indicated cell type and plotted using the indicated color scale and using *Gapdh* expression for normalization. (**F**) Schematic of experiments addressing the influence of IL-15 signaling on T cell proliferation in two tumor models. KI67^{+} OT-I cells served as a readout of cell proliferation. (**G**) Statistical analysis of KI67 expression of tumor-resident OT-I T cells in B78-ChOVA and PyMT-ChOVA tumors treated with IL-15-blocking antibody or control using a Mann-Whitney test. $^{*}P < 0.05$. Data are pooled from 2 experiments. (**H**) Statistical analysis of KI67 expression of tumor-resident OT-I T cells in B78-ChOVA tumors grown in wild-type or IL-15-deficient animals using a Mann-Whitney test. $^{***}P < 0.001$. Data are pooled from 2 experiments.

To determine whether TIL proliferation was antigen dependent, we utilized OT-I T cells in which TCR signaling can be blocked as a result of a point mutation in the proximal kinase ZAP70 (ZAP70AS) (30, 31), which renders the kinase sensitive to a custom ATP analog inhibitor, HXJ42. We transferred congenically marked OT-I/ZAP70$^{+/-}$ and OT-I/ZAP70AS cells into tumor-bearing PyMT-ChOVA hosts and

generated living slice cultures from tumors 14 days after transfer. We cultured these slices with or without HXJ42 in the presence of EdU overnight and assessed the proliferation of endogenous and OT-I T cells by flow cytometry (Figure 5A). A parallel treatment of isolated OT-I cells with HXJ42, stimulated by APCs, demonstrated that the drug indeed blocks TCR-dependent EdU incorporation (Supplemental Figure 2). However, while approximately 10% of OT-I T cells went through DNA synthesis in the tumor slice incubated overnight without inhibitor, HXJ42 blockade of ZAP70 did not reduce EdU incorporation (Figure 5, B and C). We repeated this experiment using wild-type OT-I T cells in the presence or absence of the antibody clone 25D1.16, which blocks TCR recognition by binding to the OT-I peptide-MHC complex (32). Similar to the ZAP70 inhibitor, this demonstrated that EdU incorporation of tumor-infiltrating OT-I cells did not depend on TCR recognition (Figure 5D).

The observation that T cells were undergoing proliferation despite the absence of TCR signaling suggested that the cells might be responding to other elements of the microenvironment. Dependence on antigen for survival and proliferation has been a hallmark of dysfunctional T cells in virus infection (33), whereas maintenance of memory effector T cells in sites like lymph nodes is dependent on cytokines. We considered the possibility that TILs were actively retained and perhaps even expanded as part of the tumor niche. RNA profiling data from our previous work (7) demonstrated elevated expression of multiple cytokine transcripts in tumor-infiltrating myeloid cells (Figure 5E). Among these cytokines, the common γ chain cytokine IL-15 induces T cell activation and proliferation similar to TCR signaling (34) and is specifically important in the maintenance and proliferation of memory T cells (35). We found IL-15R expression on tumor-resident T cells and responsiveness of tumor-experienced OT-I T cells in vitro to IL-15 (Supplemental Figure 3), so we sought to determine whether a component of cell-cycle entry might derive from this particular cytokine. We undertook experiments using a blocking antibody (Figure 5F) in both PyMT-ChOVA mice and in the aggressive ectopic B16 melanoma model, B78-ChOVA (7). In both cases we found modest inhibition of KI67 expression in OT-I cells, statistically significant only in the spontaneous model, after repetitive injection of antibodies during the course of the response (Figure 5G). Since in vivo antibody blockade of IL-15 may not saturate and thus fully neutralize this cytokine, particularly in the context of a dense TME, we implanted IL-15 knockout mice with B78-ChOVA tumors and transferred OT-I T cells after tumors had established. In this setting, we observed an approximately 50% reduction in the frequency of KI67 cells in tumors (Figure 5H). Although IL-15 blockade may have additional mechanisms of action, for example, possibly acting on NK cells, this result is consistent with active maintenance and expansion of TILs by a cytokine-driven mechanism.

Discussion

TILs have been a paradox — while in most human tumors tumor-reactive T cells can be found, these cells fail to elicit strong antitumor responses. How (and why) are these cells retained? Previous work has outlined a wide range of mechanisms of T cell suppression that can act in solid tumors toward programming dysfunction of these cells: metabolites made by cell types collectively described as myeloid-derived suppressor cells (36), IL-4 and IL-10 produced by TAMs (37), expression of IL-10 and TGF-β by $Foxp3^+$ regulatory CD4 T cells (38), the expression of inhibitory checkpoint signaling pathways by tumor cells (e.g., PD1/PDL1) (39), and general physiological effects of rapidly growing tissues (e.g., hypoxia and low nutrient levels; refs. 40, 41). While it may have been presumed that these aggregate and diverse signals have an immediate effect on T cell responsiveness, our study directly demonstrates that the conditioning process has phases in tumor-bearing hosts.

We found evidence that the initial interaction with TAMs that we and others had previous documented (4, 7, 11, 12) is merely the first response, likely prior to the cells being completely "dysfunctional" and likely but not definitively or solely the driver of that state. In this "phase A" of intratumoral motility, observed as early as day 4 but finished by day 10 and studied extensively here at day 14, incoming T cells display slower motility along with evidence of NUR77 upregulation and ability to produce IFN-γ and GZMB. However, we found that this does not persist, and subsequent to these engagements T cells fail to stably engage APCs or tumor cells, despite being in proximity to them. We propose to consider this second apparently antigen-independent "phase B" as the prototypical one that defines resident dysfunctional TILs. Our findings have reminiscence of the initial characterization, by multiphoton imaging, of phases of T cell motility during lymph node priming (17, 18), which has fueled ongoing works to under-

stand cell-cell interactions and the biology of T cells during each phase. We do note that the apparent lack of antigen recognition may mask weak antigen recognition, as multiple studies have documented "motile synapses" that are effective in some elements of signaling in vivo (42–44). That these late-phase interactions are likely antigen independent is supported by the apparent lack of a role for either TCR stimuli (e.g., ZAP70) or the appearance of TCR-induced signals (e.g., NUR77), although signals might be generated but are just too weak for these methods to detect.

That these observations are not experimentally contrived may be seen from the fact that we first made the observation of faster motility within the endogenous T cell repertoire and subsequently tested cells with identical TCRs with different residence times. We also excluded the competing hypothesis that the difference was due to different tumor-antigen affinity. Additionally, all of our data come from paired experiments in which two populations were compared to one another, within the same tumor, on the same day, and in the same imaging volume. We thus consider it unlikely that these observations are unique to the experimental configuration but instead propose that this behavior is a hallmark of the profound dysfunction in phase B, associated with loss of effector function, NUR77 downregulation, and changes in surface phenotype (expression of PD1, LAG3, CD244/2B4, and TIM3).

While other previous studies have observed above-background levels KI67 staining (for example, refs. 45, 46) in TILs within progressing tumors, ours takes this observation an important step further by defining it as being antigen independent and at least partially cytokine driven. Thus, while profound increases in KI67 staining in TILs, perhaps following therapies (e.g., refs. 45, 47) may indeed predict a better T cell response, our data suggest that modest levels of TIL proliferation should be interpreted carefully and that increased levels of proliferation may not necessarily mean that a better antigen-reactive T cell response is ongoing or imminent.

Adoptive T cell therapies, using expanded TILs or T cells engineered to express chimeric antigen receptors and engineered TCRs, are moving forward in clinical trials. While T cell therapy has shown tremendous success in hematological settings (48, 49), these therapies still need to demonstrate their efficacy in solid tumors in the face of an immune microenvironment that appears capable of redirecting and/or inactivating T cell effector functions (50, 51). Lymphodepletion prior to T cell administration has become a standard regimen for T cell therapies of hematological diseases, and this treatment enables the expansion of the transferred T cells due to elevated levels of the homeostatic cytokines IL-7 and IL-15 and corresponding loss of competitors for these cytokines (52). Our results indicate that lymphodepletion may benefit the treatment of solid tumors, due to a previously unappreciated maintenance of tumor-specific but dysfunctional T cells by IL-15 in situ. As these T cells occupy the TME, their presence may act as a sink for other proinflammatory cytokines as well, and their initial depletion may serve to remove this sink.

Similarly, IL-15 administration has previously shown modest but restricted promise in preclinical models by enhancing the size of the tumor-reactive T cell pool (53), and recombinant IL-15 has entered clinical testing (54). In mice, most studies investigating the activity of T cell enhancing drugs such as IL-15 have been performed with fast-growing ectopic or orthotopic tumor models (53, 55, 56). Despite their apparent advantages of speed and reliability, these tumor models lack the normal tumor development that allows for the establishment and maturation of a T cell pool prior to treatment. Our results indicate that even in the presence of a sizeable antitumor selection of TILs, IL-15 supported maintenance and proliferation of TILs, derived from the TME alone, is not enough to induce meaningful antitumor T cell responses. More importantly, our results raise the question of whether prolonged IL-15 treatment may best support incoming T and NK cells or might simply promote growth of an increasing pool of dysfunctional T cells that take up IL-15 and likely other proinflammatory cytokines and compete with more effective T cells, thereby opposing the therapeutic goals.

Methods

Mice. Mice were handled in accordance with the guidelines of the UCSF IACUC. 6- to 8-week-old C57/Bl6 animals were acquired from Simonsen, and all transgenic strains were obtained from the UCSF Rodent Program exchange unless noted otherwise. PyMT-ChOVA (4) transgenic mice were maintained by backcrossing against C57/Bl6 animals for at least 10 generations. For microscopy experiments, PyMT-ChOVA mice were crossed to human CD2-RFP (25), CX3CR1-EGFP (27), and CD11c-Cherry (28) lines maintained on a C57/Bl6 background (>10 generations). Tumor-bearing female PyMT-ChOVA mice were used at between 27 and 33 weeks of age, depending on tumor size. OT-I (Jackson) and OT-3 (26) transgenic mice (gift from Dietmar Zehn, Swiss Vaccine Research Institute, Lausanne, Switzerland) were bred to Actin-CFP and Ubiquitin-GFP

(both Jackson), human CD2-RFP, NUR77-EGFP (described in refs. 30, 57; a gift from Julie Zikherman, UCSF), and CD45.1 (Jackson) lines that have been maintained on a C57/Bl6 background for more than 10 generations. OT-I/ZAP70AS/CD45.1 and OT-I/ZAP70$^{+/-}$/CD45.1 animals were described previously (30, 57) and were a gift from Art Weiss (UCSF). IL-15 knockout animals were a gift from Shomyseh Sanjabi (UCSF). Female mice 6–10 weeks of age served as T cell donors. 6- to 10-week-old C57/Bl6 male animals and IL-15$^{-/-}$ mice of mixed gender served as hosts for ectopic tumor experiments.

Analysis of T cell function in tumor models. PyMT-ChOVA mice were used for intravital imaging when tumors were palpable near the inguinal lymph node, and functional assays were performed in mice with visible tumors. In some cases, 10 μg anti-mouse IL-15 antibody was injected i.p. twice weekly, beginning the day prior to T cell infusion (clone M96, gift from Heather Arnett, Amgen). For all experiments with PyMT animals, 5×10^6 naive OT-I T cells were transferred to tumor-bearing hosts and analysis was performed 4 or 14 days after injection. B78.ChOVA (4) and tumor cells were cultured under standard culture conditions. Cells were harvested and washed 3 times with PBS and then mixed at a 1:1 ratio with growth factor–reduced Matrigel Matrix (BD Biosciences) for a final injection volume of 50 μl. 1×10^5 B78.ChOVA tumor cells were injected in the right flank of shaved mice subcutaneously. For B78.ChOVA-bearing hosts 1×10^6 naive OT-I T cells were injected 4 days after tumor inoculation and analyzed 14 days later.

Two-photon tumor imaging and analysis. Tumor-bearing mice were kept under anesthesia using isofluorane and injected with 10 μg Evans Blue in PBS before surgery by retro-orbital injection. Mammary tumors were surgically exposed and in some cases treated with 20 μM CellEvent (Invitrogen) in PBS for 30 minutes before imaging. Two-photon imaging was performed using a custom-built instrument equipped with 2 Ti-Sapphire lasers and 6 acquisition channels: laser 1, MaiTai laser (Spectra-Physics) tuned to 870 nm (CFP, GFP, Evans) or 910 nm (GFP, Evans Blue); Laser 2, DeepSee II (Coherent) tuned to 1,030 nm (CellEvent Green [Invitrogen], RFP/Cherry). In some cases alternating laser emission with collection of 12 channels was used in order to separate second harmonic signals of the 1,030-nm line from GFP emission. Time-lapse videos were acquired at a frame rate of every minute at a z-resolution of 3 μm. Data were analyzed using FIJI, Imaris (Bitplane), and MATLAB (Mathworks). FIJI algorithms were used for image reconstruction and drift stabilization. Imaris was used for video generation, cell surface detection, and generation of cell speed and mean track speed data. MATLAB scripts were used to visualize track patterns for the rosette plots and to analyze tracks for arrest coefficients. Arrest was defined as cell speed under 2 μm/min for more than 2 minutes.

Ex vivo tumor slice cultures. PyMT-ChOVA animals were injected with naive OT-I T cells, and tumors were dissected 14 days later. Tumors were kept in ice-cold RPMI until sectioning was completed. Tumors were embedded in 2% ultra-low-melting type agarose (SeaPlaque), and 300-μM sections were prepared using a Compresstome VF-200 (Precisionary Instruments). Slices were fixed to plastic coverslips using Vetbond (3M) and cultured in RPMI/10% FCS supplemented with 10 μM EdU (Invitrogen) for 16–20 hours before analysis. Tumor slices were treated with 1 μM HXJ42 ZAP70 inhibitor (a gift from Art Weiss) or 25 μg/ml anti-SL8 (clone 25-D1.16, eBioscience).

Tumor cell preparation. Tumors and tumor slices were finely chopped in RPMI medium, washed with PBS/10 mM EDTA, and resuspended in RPMI supplemented with 0.1 mg/ml Liberase TL (Roche) and 0.2 mg/ml DNaseI (Roche). In some cases, 25 μg/ml Liberase TM (Roche) or mixes of 100 U/ml Collagenase I and 500 U/ml Collagenase IV (Worthington) were used instead. All enzyme concentrations were titrated on in vitro–activated OT-I T cells to ensure retention of surface marker staining on T cells. Digests were performed at 37°C on an orbital shaker rotating at 200 rpm, and dissociated cells were separated from tumor chunks using cell strainers by washing with PBS/10 mM EDTA. Tumor tissue was digested up to 3 times. Lymph node cells were prepared in the same way.

Flow cytometry. Cells from tumor digests were stained in ice-cold PBS supplemented with 2% FCS, 2 mM EDTA, and 0.1% NaN_3. If cells were used for further experiments, NaN_3 was replaced by 100 U/ml Penicillin/Streptomycin (Gibco). Cells were stained in the presence of Fc-blocking reagents, using either 5% rat serum (StemCell Technologies) or 10 μg/ml anti-mouse CD16/32 antibody (UCSF Antibody Core Facility). Dead cells were labeled using Zombie NIR LiveDead (BioLegend) before fixation and intracellular staining using the FoxP3 staining buffer kit (eBioscience). EdU staining was performed using ClickiT EdU kits (Invitrogen). The following antibodies were acquired from eBiosciences: CD4 (GK1.5), CD8 (53-6.7), CD11B (M1/70), CD25 (PC61), CD44 (IM7), CD45 (30-F11), CD45.1 (A20), CD45.2 (104), CD90.2 (30-H12), CD160 (7H1), CD215/IL-15RA (DNT15Ra), CD223/LAG3 (C9B7W), CD279/PD1 (RMP1-30), CD326/EPCAM (G8.8),

KLRG-1 (2F1), TIM3 (RMT3-23), IFN-γ (XMG1.2), GZMB (GB11), and KI67 (SolA15). Antibody against CD244.2/2B4 [m2B4 (B6)458.1] was from BioLegend. Samples were assessed on a Fortessa LSRII (BD Bioscience). CD8 TILs were defined as $CD45^+$, $CD11b^-$, $CD90.2^+$, $CD4^-$, $CD8^+$, and $CD44^+$.

Intracellular cytokine staining. $CD8^+$ T cells were enriched from tumor digests using CD8-negative enrichment kits (StemCell Technologies), supplemented with 1 μg/ml biotinylated anti-mouse CD326 (eBioscience) antibody to remove tumor cells. Cells were incubated with RPMI/10% FCS supplemented with 10 μg/ml Brefeldin A (Cayman Chemical) and Monensin (BioLegend) at 37°C/5% CO_2 for 4 hours in the presence or absence of 10 ng/ml PMA and 0.5 μg/ml ionomycin. Cells were labeled with Zombie NIR LiveDead (BioLegend) before fixation using the FoxP3 Staining Kit (eBioscience) and subsequent intracellular staining for cytokines and surface markers.

In vitro T cell cultures. Splenocytes or BMDCs of wild-type mice were loaded with 100 ng/ml SIINFEKL peptide (eBioscience) in RPMI/10% FCS for 30 minutes and mixed with lymph node cells from OT-I transgenic mice. Cells were supplemented with 10 U/ml human IL-2 (Peprotech) every second day of culture. Cells were used 4–6 days after culture initiation.

In vitro BMDC generation. Femurs of wild-type mice were flushed and cultured in IMDM supplemented with 10% FCS and GMCSF. Two days prior to experiments, cells differentiation was induced by the addition of IL-4 to the medium. Cells were activated by the addition of LPS 12 hours prior to the experiment. Cells were used 7–13 days after culture initiation.

Statistics. All statistical analysis was performed using Prism 6 Software (Graphpad) and is represented as mean ± SEM. Nonparametric unpaired 2-tailed Kolmogorov-Smirnov *t* tests were used for the analysis between two groups, whereas nonparametric 1-way ANOVA Kruskal-Wallis tests were used when multiple groups were compared. When paired data were analyzed, nonparametric paired Wilcoxon rank *t* tests were used. In all experiments, *P* values of less than 0.05 were considered significant.

Study approval. All experiments conformed to ethical principles and guidelines approved by the UCSF IACUC.

Author contributions

BB and MFK conceived of the experiments. BB performed the experiments with assistance from AN and analyzed results. BB assembled the data and figures. BB and MFK wrote the manuscript.

Acknowledgments

We thank Pete Beemiller for programming of image analysis scripts; Mark Headley for help with video encoding; Heather Arnett (Amgen) for anti-IL-15; Byron Au-Yeung and Art Weiss for providing ZAP70AS mice, titrated reagents, and advice; and Sebastian Peck, Kaitlin Corbin, and Henry Pinkard for imaging support. This work was funded by an EMBO postdoctoral fellowship (to BB), by the National Cancer Institute (to MFK), and by the Mediterranean Institute for Advanced Study for writing support (to MFK).

Address correspondence to: Matthew F. Krummel, 513 Parnassus Avenue, San Francisco, California 94143-0511, USA. Phone: 415.514.3130; E-mail: matthew.krummel@ucsf.edu.

BB's present address is: Pfizer Inc., South San Francisco, California, USA.

1. Hellström I, Hellström KE, Pierce GE, Yang JP. Cellular and humoral immunity to different types of human neoplasms. *Nature*. 1968;220(5174):1352–1354.
2. Wherry EJ, et al. Molecular signature of CD8+ T cell exhaustion during chronic viral infection. *Immunity*. 2007;27(4):670–684.
3. Baitsch L, et al. Exhaustion of tumor-specific CD8+ T cells in metastases from melanoma patients. *J Clin Invest*. 2011;121(6):2350–2360.
4. Engelhardt JJ, et al. Marginating dendritic cells of the tumor microenvironment cross-present tumor antigens and stably engage tumor-specific T cells. *Cancer Cell*. 2012;21(3):402–417.
5. Gubin MM, et al. Checkpoint blockade cancer immunotherapy targets tumour-specific mutant antigens. *Nature*. 2014;515(7528):577–581.
6. Gros A, et al. PD-1 identifies the patient-specific CD8+ tumor-reactive repertoire infiltrating human tumors. *J Clin Invest*. 2014;124(5):2246–2259.
7. Broz ML, et al. Dissecting the tumor myeloid compartment reveals rare activating antigen-presenting cells critical for T cell immunity. *Cancer Cell*. 2014;26(5):638–652.
8. Roberts EW, et al. Critical role for CD103(+)/CD141(+) dendritic cells bearing CCR7 for tumor antigen trafficking and priming

of T cell immunity in melanoma. *Cancer Cell*. 2016;30(2):324–336.
9. Yee C, Savage PA, Lee PP, Davis MM, Greenberg PD. Isolation of high avidity melanoma-reactive CTL from heterogeneous populations using peptide-MHC tetramers. *J Immunol*. 1999;162(4):2227–2234.
10. Lee PP, et al. Characterization of circulating T cells specific for tumor-associated antigens in melanoma patients. *Nat Med*. 1999;5(6):677–685.
11. Bauer CA, Kim EY, Marangoni F, Carrizosa E, Claudio NM, Mempel TR. Dynamic Treg interactions with intratumoral APCs promote local CTL dysfunction. *J Clin Invest*. 2014;124(6):2425–2440.
12. Boissonnas A, et al. CD8+ tumor-infiltrating T cells are trapped in the tumor-dendritic cell network. *Neoplasia*. 2013;15(1):85–94.
13. Gattinoni L, Powell DJ, Rosenberg SA, Restifo NP. Adoptive immunotherapy for cancer: building on success. *Nat Rev Immunol*. 2006;6(5):383–393.
14. Krummel MF, Bartumeus F, Gérard A. T cell migration, search strategies and mechanisms. *Nat Rev Immunol*. 2016;16(3):193–201.
15. Negulescu PA, Krasieva TB, Khan A, Kerschbaum HH, Cahalan MD. Polarity of T cell shape, motility, and sensitivity to antigen. *Immunity*. 1996;4(5):421–430.
16. Dustin ML, Bromley SK, Kan Z, Peterson DA, Unanue ER. Antigen receptor engagement delivers a stop signal to migrating T lymphocytes. *Proc Natl Acad Sci USA*. 1997;94(8):3909–3913.
17. Miller MJ, Wei SH, Parker I, Cahalan MD. Two-photon imaging of lymphocyte motility and antigen response in intact lymph node. *Science*. 2002;296(5574):1869–1873.
18. Mempel TR, Henrickson SE, Von Andrian UH. T-cell priming by dendritic cells in lymph nodes occurs in three distinct phases. *Nature*. 2004;427(6970):154–159.
19. Friedman RS, Beemiller P, Sorensen CM, Jacobelli J, Krummel MF. Real-time analysis of T cell receptors in naive cells in vitro and in vivo reveals flexibility in synapse and signaling dynamics. *J Exp Med*. 2010;207(12):2733–2749.
20. Beemiller P, Jacobelli J, Krummel MF. Integration of the movement of signaling microclusters with cellular motility in immunological synapses. *Nat Immunol*. 2012;13(8):787–795.
21. Moreau HD, et al. Dynamic in situ cytometry uncovers T cell receptor signaling during immunological synapses and kinapses in vivo. *Immunity*. 2012;37(2):351–363.
22. Woolf E, et al. Lymph node chemokines promote sustained T lymphocyte motility without triggering stable integrin adhesiveness in the absence of shear forces. *Nat Immunol*. 2007;8(10):1076–1085.
23. Overstreet MG, et al. Inflammation-induced interstitial migration of effector CD4+ T cells is dependent on integrin αV. *Nat Immunol*. 2013;14(9):949–958.
24. Friedman RS, Jacobelli J, Krummel MF. Surface-bound chemokines capture and prime T cells for synapse formation. *Nat Immunol*. 2006;7(10):1101–1108.
25. Veiga-Fernandes H, et al. Tyrosine kinase receptor RET is a key regulator of Peyer's patch organogenesis. *Nature*. 2007;446(7135):547–551.
26. Enouz S, Carrié L, Merkler D, Bevan MJ, Zehn D. Autoreactive T cells bypass negative selection and respond to self-antigen stimulation during infection. *J Exp Med*. 2012;209(10):1769–1779.
27. Jung S, et al. Analysis of fractalkine receptor CX(3)CR1 function by targeted deletion and green fluorescent protein reporter gene insertion. *Mol Cell Biol*. 2000;20(11):4106–4114.
28. Khanna KM, Blair DA, Vella AT, McSorley SJ, Datta SK, Lefrançois L. T cell and APC dynamics in situ control the outcome of vaccination. *J Immunol*. 2010;185(1):239–252.
29. Thompson ED, Enriquez HL, Fu YX, Engelhard VH. Tumor masses support naive T cell infiltration, activation, and differentiation into effectors. *J Exp Med*. 2010;207(8):1791–1804.
30. Au-Yeung BB, et al. A genetically selective inhibitor demonstrates a function for the kinase Zap70 in regulatory T cells independent of its catalytic activity. *Nat Immunol*. 2010;11(12):1085–1092.
31. Au-Yeung BB, et al. Quantitative and temporal requirements revealed for Zap70 catalytic activity during T cell development. *Nat Immunol*. 2014;15(7):687–694.
32. Kim JV, Kang SS, Dustin ML, McGavern DB. Myelomonocytic cell recruitment causes fatal CNS vascular injury during acute viral meningitis. *Nature*. 2009;457(7226):191–195.
33. Wherry EJ, Kurachi M. Molecular and cellular insights into T cell exhaustion. *Nat Rev Immunol*. 2015;15(8):486–499.
34. Liu K, Catalfamo M, Li Y, Henkart PA, Weng NP. IL-15 mimics T cell receptor crosslinking in the induction of cellular proliferation, gene expression, and cytotoxicity in CD8+ memory T cells. *Proc Natl Acad Sci USA*. 2002;99(9):6192–6197.
35. Surh CD, Sprent J. Homeostasis of naive and memory T cells. *Immunity*. 2008;29(6):848–862.
36. Gabrilovich DI, Ostrand-Rosenberg S, Bronte V. Coordinated regulation of myeloid cells by tumours. *Nat Rev Immunol*. 2012;12(4):253–268.
37. Noy R, Pollard JW. Tumor-associated macrophages: from mechanisms to therapy. *Immunity*. 2014;41(1):49–61.
38. Shevach EM. Mechanisms of foxp3+ T regulatory cell-mediated suppression. *Immunity*. 2009;30(5):636–645.
39. Ostrand-Rosenberg S, Horn LA, Haile ST. The programmed death-1 immune-suppressive pathway: barrier to antitumor immunity. *J Immunol*. 2014;193(8):3835–3841.
40. MacIver NJ, Michalek RD, Rathmell JC. Metabolic regulation of T lymphocytes. *Annu Rev Immunol*. 2013;31:259–283.
41. Chang CH, et al. Metabolic Competition in the tumor microenvironment is a driver of cancer progression. *Cell*. 2015;162(6):1229–1241.
42. Marangoni F, et al. The transcription factor NFAT exhibits signal memory during serial T cell interactions with antigen-presenting cells. *Immunity*. 2013;38(2):237–249.
43. Azar GA, Lemaître F, Robey EA, Bousso P. Subcellular dynamics of T cell immunological synapses and kinapses in lymph nodes. *Proc Natl Acad Sci U S A*. 2010;107(8):3675–3680.
44. Friedman RS, Beemiller P, Sorensen CM, Jacobelli J, Krummel MF. Real-time analysis of T cell receptors in naive cells in vitro and in vivo reveals flexibility in synapse and signaling dynamics. *J Exp Med*. 2010;207(12):2733–2749.
45. Bos PD, Plitas G, Rudra D, Lee SY, Rudensky AY. Transient regulatory T cell ablation deters oncogene-driven breast cancer and enhances radiotherapy. *J Exp Med*. 2013;210(11):2435–2466.

46. Kovacsovics-Bankowski M, et al. Detailed characterization of tumor infiltrating lymphocytes in two distinct human solid malignancies show phenotypic similarities. *J Immunother Cancer*. 2014;2(1):38.
47. Shuford WW, et al. 4-1BB costimulatory signals preferentially induce CD8+ T cell proliferation and lead to the amplification in vivo of cytotoxic T cell responses. *J Exp Med*. 1997;186(1):47–55.
48. Maude SL, et al. Chimeric antigen receptor T cells for sustained remissions in leukemia. *N Engl J Med*. 2014;371(16):1507–1517.
49. Garfall AL, et al. Chimeric antigen receptor T cells against CD19 for multiple myeloma. *N Engl J Med*. 2015;373(11):1040–1047.
50. Katz SC, et al. Phase I hepatic immunotherapy for metastases study of intra-arterial chimeric antigen receptor-modified T-cell therapy for CEA+ liver metastases. *Clin Cancer Res*. 2015;21(14):3149–3159.
51. Ahmed N, et al. Human epidermal growth factor receptor 2 (HER2) -specific chimeric antigen receptor-modified T cells for the immunotherapy of HER2-positive sarcoma. *J Clin Oncol*. 2015;33(15):1688–1696.
52. Rosenberg SA, Restifo NP. Adoptive cell transfer as personalized immunotherapy for human cancer. *Science*. 2015;348(6230):62–68.
53. Epardaud M, et al. Interleukin-15/interleukin-15R alpha complexes promote destruction of established tumors by reviving tumor-resident CD8+ T cells. *Cancer Res*. 2008;68(8):2972–2983.
54. Conlon KC, et al. Redistribution, hyperproliferation, activation of natural killer cells and CD8 T cells, and cytokine production during first-in-human clinical trial of recombinant human interleukin-15 in patients with cancer. *J Clin Oncol*. 2015;33(1):74–82.
55. Rhode PR, et al. Comparison of the superagonist complex, ALT-803, to IL-15 as cancer immunotherapeutics in animal models. *Cancer Immunol Res*. 2016;4(1):49–60.
56. Kim PS, et al. IL-15 superagonist/IL-15RαSushi-Fc fusion complex (IL-15SA/IL-15RαSu-Fc; ALT-803) markedly enhances specific subpopulations of NK and memory CD8+ T cells, and mediates potent anti-tumor activity against murine breast and colon carcinomas. *Oncotarget*. 2016;7(13):16130–16145.
57. Au-Yeung BB, et al. A sharp T-cell antigen receptor signaling threshold for T-cell proliferation. *Proc Natl Acad Sci U S A*. 2014;111(35):E3679–E3688.